

Contents lists available at [SciVerse ScienceDirect](http://SciVerse.Sciencedirect.com)

# Biochimica et Biophysica Acta

journal homepage: [www.elsevier.com/locate/bbamem](http://www.elsevier.com/locate/bbamem)

## Membrane defects enhance the interaction of antimicrobial peptides, aurein 1.2 versus caerin 1.1

David I. Fernandez <sup>a</sup>, Marc-Antoine Sani <sup>a</sup>, Andrew J. Miles <sup>b</sup>, B.A. Wallace <sup>b</sup>, Frances Separovic <sup>a,\*</sup><sup>a</sup> School of Chemistry, Bio21 Institute, University of Melbourne, VIC 3010, Australia<sup>b</sup> Institute of Structural and Molecular Biology, Birkbeck College, University of London, London WC1E 7HX, UK

### ARTICLE INFO

#### Article history:

Received 1 January 2013

Received in revised form 5 March 2013

Accepted 8 March 2013

Available online 15 March 2013

#### Keywords:

Antimicrobial peptide  
 Model membrane  
 Peptide–lipid interaction  
 Lipid domain  
 Circular dichroism  
 Solid-state NMR

### ABSTRACT

The membrane interactions of the antimicrobial peptides aurein 1.2 and caerin 1.1 were observed by <sup>31</sup>P and <sup>2</sup>H solid-state NMR and circular dichroism spectroscopy. Both peptides were relatively unstructured in water. In the presence of dimyristoylphosphatidylcholine (DMPC) and mixed DMPC and dimyristoylphosphatidylglycerol (DMPG) vesicles, both peptides displayed a considerable increase in helical content with the shorter aurein peptide having a higher  $\alpha$ -helix content in both lipid systems. In fluid phase DMPC vesicles, the peptides displayed differential interactions: aurein 1.2 interacted primarily with the bilayer surface, while the longer caerin 1.1 was able to penetrate into the bilayer interior. Both peptides displayed a preferential interaction with the DMPG component in DMPC/DMPG bilayers, with aurein 1.2 limited to interaction with the surface and caerin 1.1 able to penetrate into the bilayer and promote formation of a mixture of lipid phases or domains. In gel phase DMPC vesicles, aurein 1.2 disrupted the bilayer apparently through a carpet mechanism, while no additional interaction was seen with caerin 1.1. Although a lamellar bilayer was retained with the mixed DMPC/DMPG vesicles below the phase transition, both caerin 1.1 and aurein 1.2 promoted disruption of the bilayer and formation of an isotropic phase. The peptide interaction was enhanced relative to the fluid phase and was likely driven by co-existence of membrane defects. This study thus demonstrates that the effects of the lipid phase and domains need to be considered when studying membrane interactions of antimicrobial peptides.

© 2013 Elsevier B.V. All rights reserved.

### 1. Introduction

Aurein 1.2 (GLFDIIKIAESF-NH<sub>2</sub>) and caerin 1.1 (GLLSVLGSAKHH LPHVVPVIAEHL-NH<sub>2</sub>) are two antimicrobial peptides (AMP) expressed in the skin secretions of the *Litoria* genus of Australian tree frogs [1–6]. Both peptides are cationic and fold into amphipathic  $\alpha$ -helices on partitioning into membrane mimetic environments [3,7,8]. Each peptide has been shown to be active towards numerous micro-organisms [6] as well as possessing anticancer [1,3,9] and antiviral [10,11] activities.

Previous studies conducted on these and other related peptides report that they likely exert their mode of action through direct interaction with and perturbation of the bacterial membrane [1,7,12–15]. Two principal modes of action have been proposed [16,17]: transmembrane pore formation across the membrane by either a barrel-stave [17,18] or toroidal pore [19]; or a carpet mechanism where the membrane is lysed in a detergent-like manner [16–18,20]. Aurein 1.2 with 13 residues is too short to fully span a typical phospholipid bilayer as an  $\alpha$ -helix and we have previously shown that it acts via the carpet mechanism of membrane lysis [21]. By contrast, caerin 1.1 with 25

residues would be able to fully span a membrane bilayer as an  $\alpha$ -helix and may act via a pore formation mechanism or even the carpet mechanism.

As part of a larger family of related frog AMPs, both show an increased affinity for anionic membrane systems [15,22], which has been recognised as an important determinant for activity towards micro-organisms. Biological membranes are heterogeneous and vary in composition between species, and as a function of growth cycle and environmental conditions, so model membranes have been chosen to mimic some of the desired characteristics of eukaryotic and prokaryotic membranes. Phosphatidylcholine (PC) lipids are common within eukaryotic organisms [23,24] while, despite variations between species, bacterial membranes tend to contain lipids with anionic headgroups that are effectively mimicked by phosphatidylglycerol (PG) [25]. Yet with many systems, the specific lipid phase present has been shown to modulate peptide–membrane interactions. AMP studies have usually focussed on the use of fluid (L<sub>α</sub>) phase lipid membranes but certain antimicrobial peptides, such as magainin 2, maculatin 1.1 [26] and the membrane-lytic peptide melittin, have been shown to have enhanced interactions with gel phase lipid systems [26–33].

However, studies of AMP–membrane interactions have usually concentrated on the effects of membrane charge on mediating peptide–lipid interaction rather than other structural features such as the lipid phase. Also, despite studies showing that features present in mixed

\* Corresponding author. Tel.: +61 3 8344 7137; fax: +61 3 9347 8159.  
 E-mail address: [fs@unimelb.edu.au](mailto:fs@unimelb.edu.au) (F. Separovic).

lipid phases, such as the ordered/disordered  $P_{\beta}$  ripple phase, act to promote peptide interaction [29,33–35], peptide interactions are commonly investigated using fluid lamellar bilayers. Several studies have been conducted with aurein 1.2 and caerin 1.1 showing that they act via different modes of interaction. However, the interaction has sometimes been observed to differ between measurement techniques such as quartz crystal microbalance with dissipation (QCM-D) [36] and dual polarisation interferometry (DPI) [37] using gel phase bilayers and those conducted in the fluid phase such as NMR [38]. Therefore, the effects of the lipid membrane phase on antimicrobial action required further investigation. In this study we compared and contrasted the mode of action of aurein 1.2 and a larger related AMP, caerin 1.1, which is capable of spanning a membrane bilayer and may act via a pore-forming mechanism. The peptide secondary structure was determined by circular dichroism (CD) spectroscopy and the interactions with membranes above and below the gel–fluid transition temperature were examined with  $^2\text{H}$  and  $^{31}\text{P}$  NMR spectroscopy.

## 2. Materials and methods

### 2.1. Preparation of peptide–lipid NMR samples

Perdeuterated-acyl chain dimyristoylphosphatidylcholine ( $d_{54}$ -DMPC) and natural abundance dimyristoylphosphatidylglycerol (DMPG) were purchased from Avanti Polar Lipids (Alabaster, AL, USA), and used without further purification. Aurein 1.2 and caerin 1.1 were obtained from Mimotopes (Melbourne, Australia) with purity of >90%. HCl solution (5 mM) was added before each peptide was lyophilised to ensure that any traces of trifluoroacetic acid were removed [39]. Pure  $d_{54}$ -DMPC and mixed  $d_{54}$ -DMPC/DMPG (2:1 mole ratio) lipid systems were prepared as described below and peptide added at 10:1 lipid/peptide (L/P) molar ratio. Typically 1 mg of peptide and 4 mg of phospholipid were used.

Phospholipids were dissolved in chloroform/methanol (~9:1 v/v) and a rotary evaporator used to form a thin film before samples were placed under a high vacuum overnight to remove trace amounts of solvent. Dried lipid thin films were hydrated with typically 500  $\mu\text{L}$  of Milli-Q water before being lyophilised. The dried samples were re-hydrated with typically 100  $\mu\text{L}$  of 10 mM MOPS (3-(N-morpholino) propanesulfonic acid) buffer pH 7, with or without dissolved peptide, and subjected to 5 cycles of freeze–thaw before being transferred into 5 mm NMR glass sample tubes.

### 2.2. Solid-state NMR experiments

Static deuterium and phosphorus spectra were acquired at four temperatures: with the bearing air supply to the NMR probe set to 30, 20, and 15 °C and then reheated to 30 °C. The NMR probe containing the samples was removed from the magnetic field between each temperature change and allowed to equilibrate for a minimum of 1 h and then allowed to equilibrate within the magnet for 15–20 min before spectra were collected.

$^2\text{H}$  spectra were carried out at 46.09 MHz on a Varian Inova-300 spectrometer (Palo Alto, USA) with 5 mm HX probe using a composite pulse solid echo sequence [40]. Operating conditions included 4.1  $\mu\text{s}$  90° pulses, 40  $\mu\text{s}$  echo delay and 0.5 s recycle time. Typically 20 K scans were collected and Fourier transformed using zero-filling to 16 K points with 200 Hz exponential line broadening. Oriented spectra were generated by dePacking in the time domain using a recently developed in house nmrPipe macro (unpublished data, JD Gehman). The dePacked spectrum was fit with Gaussian lineshapes and converted to order parameters by dividing the static splitting of each 26 myristoyl  $\text{CD}_2$  position with the static coupling constant of 168 kHz [41].

$^{31}\text{P}$  solid-state NMR experiments were performed at 121.543 MHz on a Varian Inova-300 spectrometer (Palo Alto, USA) with 5 mm HX probe using a Hahn echo pulse sequence with 50 kHz proton

decoupling [42]. Typically 4.4  $\mu\text{s}$  90° pulse was used with 29  $\mu\text{s}$  echo time and 3 s recycle delay. A minimum of 20 K scans was collected and processed with 100 Hz exponential line broadening and zero filling to 8 K points. Static  $^{31}\text{P}$  NMR spectra were deconvoluted as previously described [43].

### 2.3. Circular dichroism (CD) spectroscopy

For CD studies, DMPC and DMPC/DMPG (2:1) were dissolved in chloroform/methanol (2:1) and peptides were dissolved in methanol (1 mg/mL) and appropriate amounts were added to a 10 mL pear shaped flask before removal of solvents by rotary evaporation to afford lipid films with and without peptide. Lipid films were then placed under high vacuum for 0.5 to 1 h. The lipid film was suspended in 0.25 mL Milli-Q water by brief vortex mixing and water bath sonication to give a constant final peptide concentration of 1 mg/mL and phospholipid/peptide mole ratios of 15:1 and 100:1. The suspension was sonicated briefly at 30 °C until translucent prior to CD spectroscopy.

CD spectra were acquired on an Aviv spectropolarimeter (Lake-wood, NJ, USA). Peptide solutions were loaded into a 0.1 mm Suprasil quartz circular demountable cell (Hellma Ltd., UK) and spectra recorded in the wavelength range from 280 nm to 180 nm with an interval of 1 nm, and an averaging time of 2 s. Samples were allowed to equilibrate for 5 min at 30 °C prior to accumulating 3 scans. Similarly, baseline spectra of lipids prepared in the same manner but without protein, were obtained. Replicate sample and baseline spectra were averaged, and the baseline subtracted from the averaged sample spectrum of the lipid background; the resulting spectra were calibrated against a spectrum of camphorsulfonic acid before conversion to units of mean residue ellipticity using mean residue weight values of 113.7 and 103.3 for aurein and caerin, respectively. To estimate the peptide secondary structure content, analyses were carried out using the DichroWeb analysis server [44]. The reference set SMP180 was used [45] and analysis performed using the CONTIN/LL algorithm [46]. The goodness of fit parameter NMRSD was used for scaling and to assess the quality of the fit [47]. The CD spectra and associated metadata are deposited in the Protein Circular Dichroism Data Bank as entries CD0004066000 (caerin) & CD0004067000 (aurein).

## 3. Results

### 3.1. Secondary structure of aurein 1.2 and caerin 1.1 by CD

The conformational changes of aurein and caerin following association with phospholipid bilayers were characterised using CD spectroscopy. Spectra were acquired at 30 °C, above the gel–liquid transition temperature of the pure lipid systems [48]. The CD spectra and calculated helical contents of aurein and caerin in water and membrane environments are shown in Fig. 1 and Table 1. In the absence of phospholipid the peptides were largely unstructured, although aurein displayed about 20% helical content.

At low lipid/peptide ratios similar to those used with NMR experiments, zwitterionic DMPC caused a significant increase (from 20% to 70%) in the helical content exhibited by aurein 1.2, whereas caerin showed only a small increase in  $\alpha$ -helix (from 8 to 20%). Possibly the less charged shorter aurein is able to interact more with the PC bilayer resulting in a more structured peptide. At the higher lipid/peptide ratio,  $\alpha$ -helical dominates the shorter peptide structure. The membrane mimetic environment promoted an  $\alpha$ -helical secondary structure, which is a typical feature of this class of compounds [1]. Caerin remained largely unstructured although the  $\alpha$ -helical content had increased (to ~40%). When in the presence of the anionic mixed (DMPC/DMPG) lipid system, both peptides become more  $\alpha$ -helical. However, the  $\alpha$ -helical content as determined by NMR in solvent or micelles is higher [3,5] as NMR favours the structured form whereas CD is the average of the free and bound peptide structures.

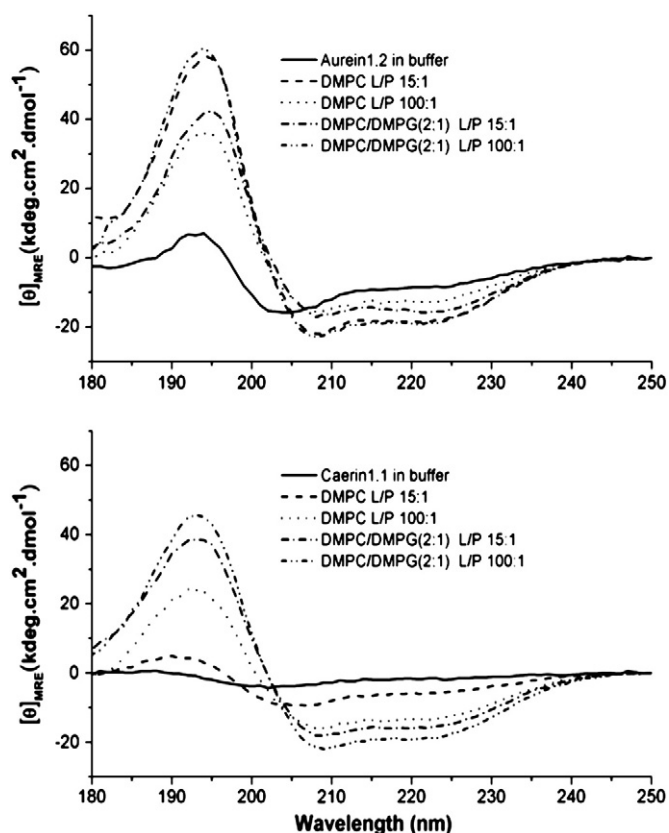


**Fig. 1.** CD spectra of aurein 1.2 (top) and caerin 1.1 (bottom) in water (solid line) and in the presence of DMPC (15:1, –) and (100:1, ...) and mixed DMPC/DMPG (2:1) (15:1, - - -) and (100:1, - - -) normalised as MRE units; 3 scans accumulated at 30 °C.

### 3.2. Peptide–lipid interactions from $^2\text{H}$ and $^{31}\text{P}$ solid-state NMR

$^2\text{H}$  NMR spectra of acyl chain deuterated phospholipid bilayers allow acyl chain order to be investigated, providing a tool to probe peptide interactions occurring within the membrane. A perdeuterated lipid acyl chain yields a spectrum with a complex lineshape (Pake powder pattern) in which alterations in splittings (width) provide an indication of changes in acyl chain order and packing [49]. Static  $^{31}\text{P}$  NMR of unoriented phospholipid bilayers provides information on the lipid phase as well as the local order and dynamics within the phosphate region of the lipid [50]. Liquid lamellar ( $L_\alpha$ ) phospholipid liposomes produce an axially symmetric powder pattern (chemical shift anisotropy, CSA) for which the overall width depends on the headgroup orientation and dynamics [51]. The CSA is used here as the width of the powder pattern. Hence a combination of  $^2\text{H}$  and  $^{31}\text{P}$  NMR experiments

**Table 1**

Secondary structures of aurein 1.2 and caerin 1.1 in DMPC and DMPC/DMPG (2:1) vesicles based on CD spectroscopy. NRMSD is a goodness-of-fit parameter between the data and the calculated structure.

Sample	P/L	% $\alpha$ -helix	% other	NRMSD
Aurein/water	–	21	79	0.160
Aurein/DMPC	1:15	74	26	0.079
	1:100	48	52	0.119
Aurein/DMPC/DMPG	1:15	60	40	0.105
	1:100	69	31	0.112
Caerin/water	–	8	92	0.122
Caerin/DMPC	1:15	20	80	0.142
	1:100	39	61	0.108
Caerin/DMPC/DMPG	1:15	43	57	0.024
	1:100	61	39	0.050

was performed to determine the effects of aurein 1.2 and caerin 1.1 on phospholipid acyl chains and headgroup perturbations over a range of temperatures. A high concentration of peptide (10:1 L/P) was used to mimic the conditions under which peptides effectively lyse phospholipid bilayers [21,37].

As reported previously [43], at 30 °C the  $d_{54}$ -DMPC control sample produced a typical fluid phase  $^2\text{H}$  order parameter profile, with rigidity decreasing from the upper acyl chains down through the terminal methyl region (Fig. S1). Addition of DMPC at a 33% molar ratio had no significant effect on the order of the DMPC acyl chains, as seen in similar lipid systems [43,52,53]. The  $^{31}\text{P}$  spectra of DMPC and mixed DMPC/DMPG vesicles (Fig. 2) consist of typical axially symmetric powder patterns at 30 °C with a CSA of  $\sim 45$  ppm for DMPC and the mixed lipid system contained a merged CSA of both DMPC and DMPG of 40 and 31 ppm, respectively (Table 2). A small peak of  $\sim 1\%$  intensity was observed at the isotropic chemical shift position in the DMPC sample which was likely caused by a small population of internal small unilamellar vesicles (observed by cryo-TEM of NMR samples, Fig. S2). The spectrum of the mixed system produced a narrower CSA, with the DMPC component reduced by  $\sim 11\%$ , indicating that the presence of DMPG permits enhanced freedom of motion among the headgroups or change in the orientation of the headgroup in response to the charged surface [38].

In the presence of aurein 1.2, the order parameters of the upper acyl chain of DMPC decreased by  $\sim 6\%$  while the acyl chain closer to the methyl was largely unchanged. An  $\sim 16\%$  reduction in the  $^{31}\text{P}$  CSA was also observed which together indicate an increase in disorder or freedom of motion among the upper chain region and headgroup, with minimal interaction with the bilayer interior. Although the  $^{31}\text{P}$  CSA was reduced by  $\sim 16\%$  with caerin 1.1, by contrast, the order parameters of the DMPC upper acyl chain region increased by between 3 and 4% while the lower acyl chain was more disordered by between 3 and 10%; which suggested peptide interaction with the surface and entire depth of the bilayer interior. The increased resolution of the splittings reflects an ordering of the lipid acyl chains by caerin in DMPC at 30 °C.

A more complex interaction was observed with the mixed  $d_{54}$ -DMPC/DMPG bilayers (Fig. 3) at 30 °C. Addition of aurein 1.2 caused a reduction of between 3 and 5% in the order parameters of the full length of the acyl chain and two  $^{31}\text{P}$  CSAs (Fig. 4a) were resolved, with a large reduction in the linewidth ( $\sim 38\%$ ) of the minor (DMPG) component. The proportions of signal did not change significantly from their initial  $\sim 2:1$  value, suggesting that the peptide interaction was primarily with the anionic DMPG.

Caerin 1.1 had a much more pronounced effect on the anionic bilayer at 30 °C with formation of a complex mixture of isotropic, gel and fluid lamellar bilayer  $^2\text{H}$  spectra. The major (DMPC enriched)  $^{31}\text{P}$  CSA component (Fig. 5a) increased slightly by 2 ppm while the minor (DMPG enriched) component CSA decreased by 5–6 ppm. The proportions of signal in each changed significantly, with the DMPC component reducing from  $\sim 68$  to 36% of the signal while the DMPG reduced from 32 to 11%. A large peak at the isotropic chemical shift was formed that contributed 53% of the signal and indicated severe bilayer disruption. The increase in the CSA of the major component closer to that of pure DMPC and the decrease in CSA of the minor component, suggest a preferential interaction with the anionic lipid. This was supported by the DMPG component signal reducing by  $\sim 65\%$  compared with 47% for the DMPC component, which implies that the large isotropic phase was enriched in DMPG. It is likely that multiple domains were formed with the peptide incorporation inducing areas of both reduced and enhanced lipid order.

### 3.3. Effect of temperature and lipid phase on peptide interaction

Reducing the temperature just below the gel–fluid phase transition of the pure lipid systems [48] to 20 °C produced  $^2\text{H}$  spectra characteristic of restricted acyl chain motion while the DMPC  $^{31}\text{P}$  spectra (Fig. 2),

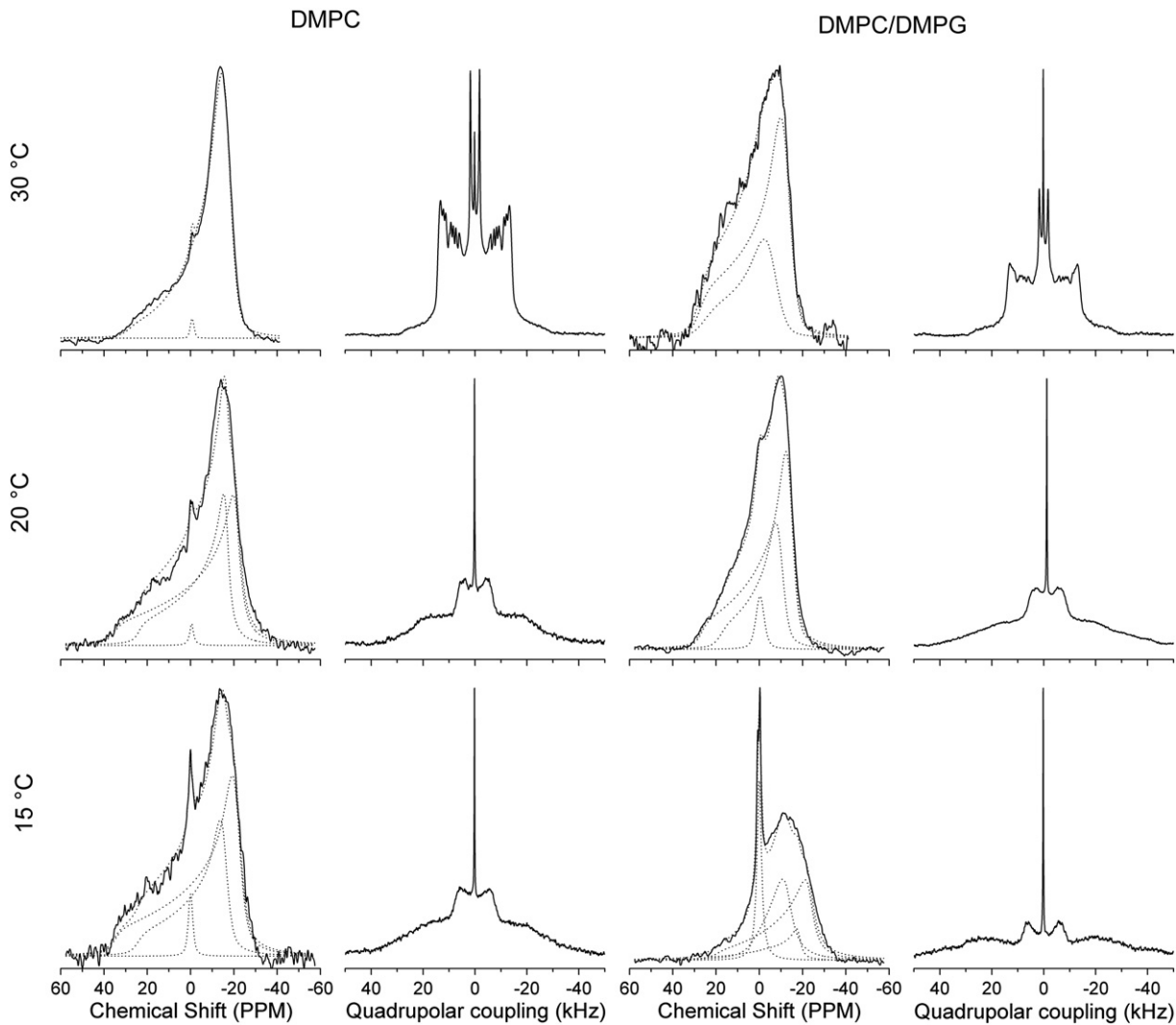


**Fig. 2.**  $^{31}\text{P}$  (1st, 3rd column) and  $^2\text{H}$  (2nd, 4th column) NMR spectra of pure  $d_{54}$ -DMPC and mixed  $d_{54}$ -DMPC/DMPG (2:1 molar ratio) lipid bilayers. Dotted lines in the  $^{31}\text{P}$  spectra represent deconvoluted components.

showed formation of a mixed phase with a 24% increase in the CSA of the major component from ~45 to ~56 ppm and a smaller proportion that exhibited an 11% reduction, which is suggestive of mixed

disordered and ordered phases such as the  $\text{P}_{\beta'}$  ripple phase [34,54]. Reducing the temperature of the DMPC/DMPG system resulted in a slight broadening of the major CSA component by 1 ppm, with the

**Table 2**

The effects of aurein 1.2 and caerin 1.1 on the  $^{31}\text{P}$  NMR lineshape<sup>a</sup> of phospholipid bilayers above and below the gel–fluid phase transition temperature.

Temperature	$^{31}\text{P}$ CSA values					
	$d_{54}$ -DMPC (ppm)			$d_{54}$ -DMPC/DMPG (2:1) (ppm)		
	Lipid bilayer	Aurein 1.2	Caerin 1.1	Lipid bilayer	Aurein 1.2	Caerin 1.1
30 °C	45.5	37.8	38.2	40.0 (68%) <sup>b</sup>	37.8 (69%)	42.0 (36%)
				31.2 (32%)	19.5 (31%)	25.9 (11%)
20 °C	56.3 (57%)	36.9 (65%)	38.5	41.0 (62%)	46.9 (57%)	54.3 (35%)
	40.4 (42%)	15.5 (30%)		27.5 (33%)	32.0 (42%)	40.7 (17%)
	Iso (1%)	Iso (5%)		Iso (5%)	Iso (1%)	21.8 (15%)
						Iso (32%)
15 °C	56.4 (61%)	Iso	54.9 (53%)	47.0 (12%)	39.0 (25%)	54.3 (35%)
	40.0 (36%)			42.5 (41%)	20.2 (23%)	41.2 (17%)
	Iso (3%)			16.2 (31%)	Iso (52%)	18.4 (16%)
				Iso (15%)		Iso (32%)
Return to 30 °C		37.1 (20%)	38.5		38.4 (41%)	54.3 (14%)
		17.6 (25%)			21.6 (44%)	37.0 (18%)
		Iso (55%)			Iso (15%)	24.7 (12%)
						Iso (56%)

<sup>a</sup> NMR measurements are to within 1 ppm.

<sup>b</sup> (%) Relative contribution to spectral intensity.

<sup>c</sup> Isotropic peak.

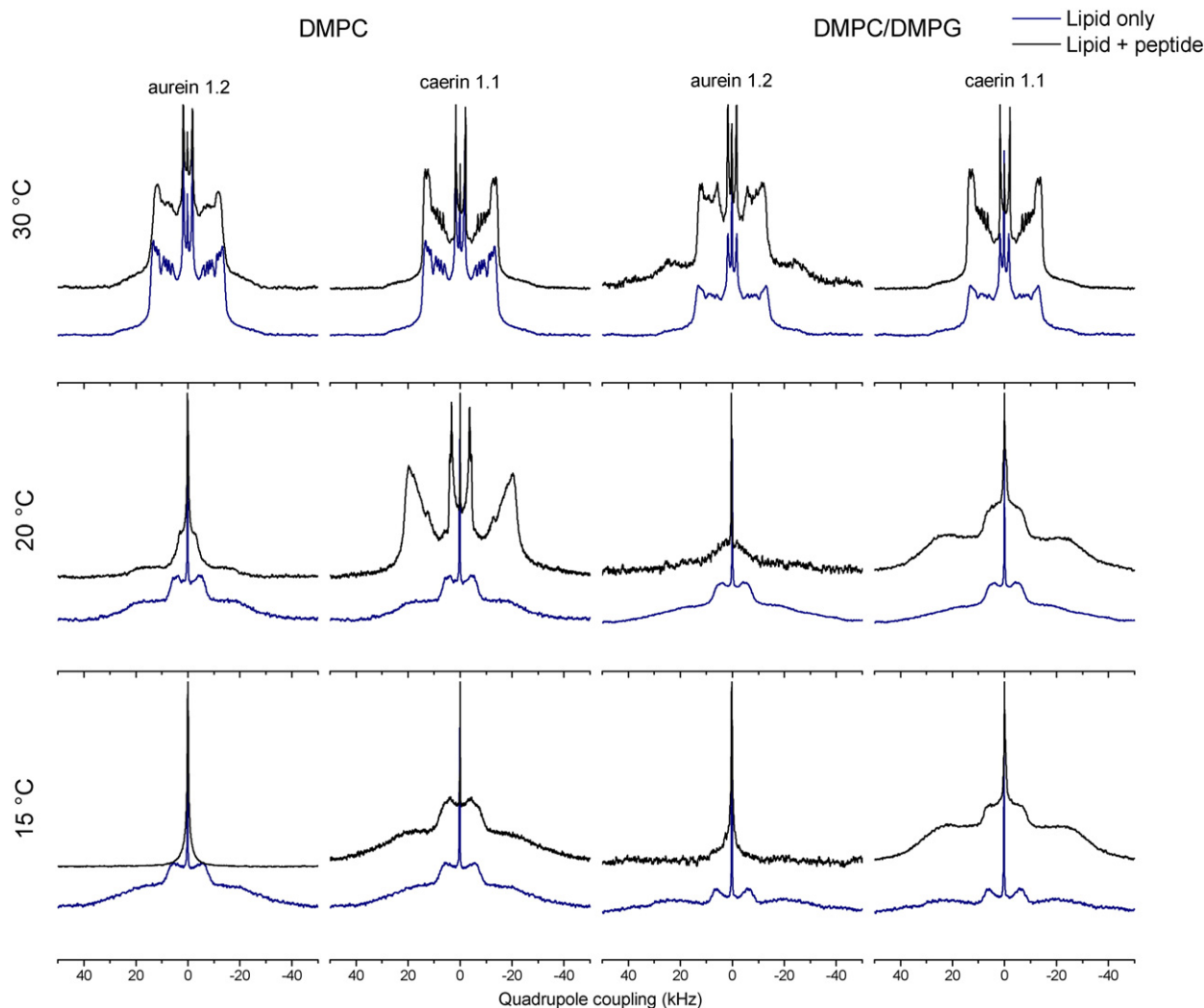


**Fig. 3.** Deuterium NMR spectra of:  $d_{54}$ -DMPC (left) and  $d_{54}$ -DMPC/DMPG (2:1) (right) lipid bilayers with aurein 1.2 (10:1) (1st, 3rd column) and caerin 1.1 (2nd, 4th column) at 30 °C, 20 °C and 15 °C. The spectra from the pure lipid are shown in the lower spectrum (blue) with the lipid + peptide spectrum vertically offset (black).

minor component reduced by 4 ppm and a small isotropic signal (5%) evident (Fig. 2, Table 2). Although similar to the DMPC system, the presence of the anionic lipid led to a more disordered system.

With aurein 1.2 in DMPC at 20 °C, the  $^2\text{H}$  spectra were indicative of more restricted acyl chain motion. The major  $^{31}\text{P}$  CSA component reduced in width by 34% while the minor component had an even more significant reduction of 61% relative to the pure lipid. Formation of small isotropic peaks in both the  $^2\text{H}$  and  $^{31}\text{P}$  spectra suggested the formation of a lipid population with severe bilayer disruption or formation of smaller tumbling structures (Figs. 3 & 4).

The  $^2\text{H}$  spectrum of DMPC with caerin 1.1 at 20 °C (Fig. 3), however, retained characteristics of a fluid phase bilayer, albeit with moderate broadening, indicating the peptide may have lowered the phase transition temperature of the bilayer. No large changes were observed in the  $^{31}\text{P}$  CSA compared to 30 °C although the lack of the ripple/gel phases observed in the pure lipid system (Fig. 2) further indicates the peptide may alter the phase transition temperature of the bilayer.

An enhanced level of bilayer disruption was observed with aurein 1.2 and the DMPC/DMPG bilayer. The  $^2\text{H}$  spectrum was a mixture of gel and isotropic phases (Fig. 3) while the  $^{31}\text{P}$  CSA of both components increased significantly to 47 and 32 ppm, respectively (Table 2). The proportion of signal present in the minor component increased from

32 to 42%, suggesting that the peptide promoted DMPG into the less ordered phase.

The interaction of caerin 1.1 with the anionic system was more pronounced with the formation of multiple lipid phases. The complex mixed, gel, fluid and isotropic  $^2\text{H}$  spectrum at 30 °C gave way to a mainly gel phase spectrum with a small isotropic signal (Fig. 3). A broad 54 ppm  $^{31}\text{P}$  CSA formed consistent with the presence of a large proportion of an immobilised/ordered lipid phase, while a smaller proportion appeared to be fluid bilayer or a more ordered DMPG-enriched phase. Another, significantly more disordered phase was also present and may have been due to components from what was previously an isotropic phase. The proportion of signal at the isotropic chemical shift decreased from 53 to 32% suggesting that a major fraction of the lipid was frozen into a more immobile state and that the isotropic fraction was highly disordered lipid since the reduction in temperature would not significantly restrict the motion of any small isotropically tumbling aggregates (especially since the  $^2\text{H}$  spectrum shows the presence of gel-phase).

A further reduction in temperature to 15 °C did not cause any significant changes in the  $^2\text{H}$  or  $^{31}\text{P}$  spectra of the pure DMPC (Fig. 2). In the anionic mixed lipid system, the reduction in temperature resulted in multiple lipid phases or domains, with a small increase in the main

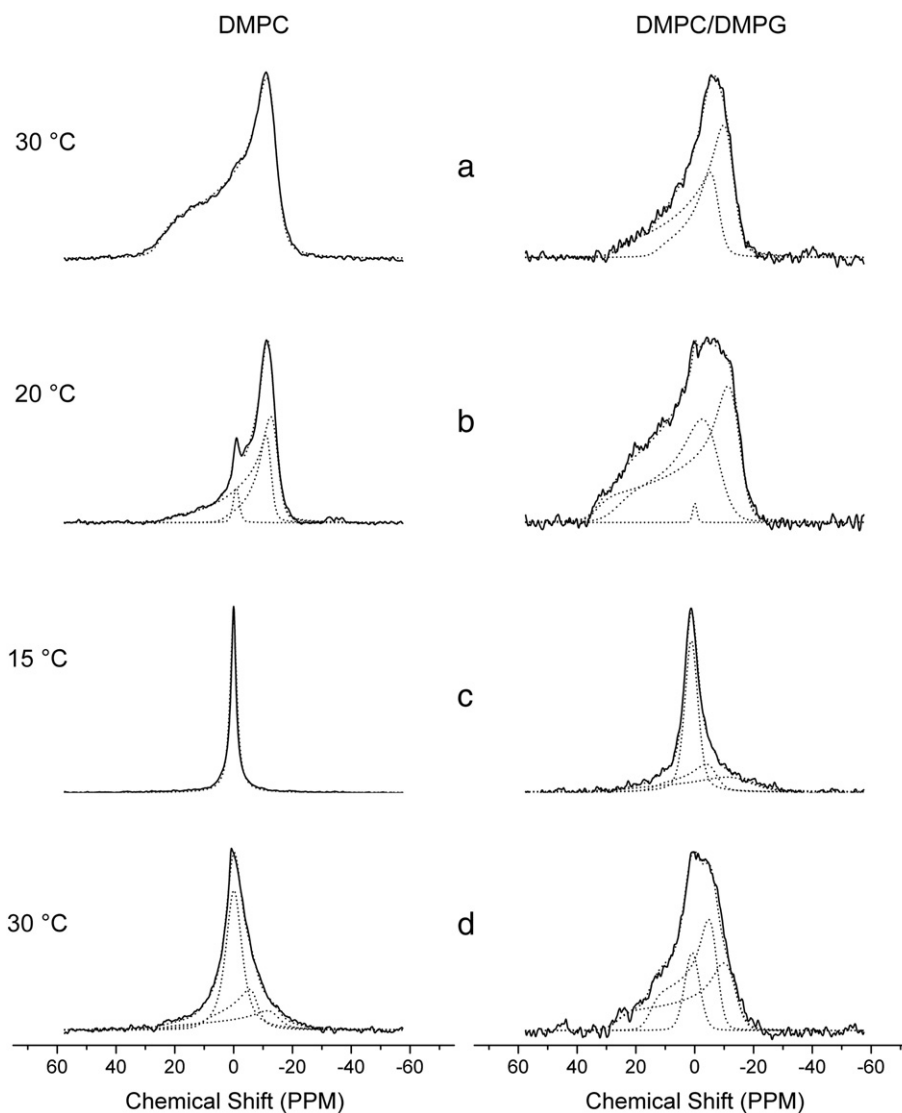


**Fig. 4.**  $^{31}\text{P}$  NMR spectra of DMPC (left) and DMPC/DMPG (2:1) (right) with aurein 1.2 at a 10:1 L/P ratio. Spectra were recorded at (a) 30 °C, (b) cooled to 20 °C, (c) further cooled to 15 °C, and (d) after reheated back to 30 °C. Unbroken lines represent the experimental spectra; dotted lines represent the deconvoluted components.

CSA from 41 to 42 ppm and reduction in fraction of the signal from ~62 to ~42%. The second major component conversely experienced a significant (11 ppm) reduction in CSA with only a slight decrease in fraction of the signal. The isotropic fraction increased from 5 to 15% and a third, broader CSA (47 ppm) was apparent with 12% of the signal.

DMPC with aurein 1.2 (Figs. 3, 4c) led to fully isotropic  $^2\text{H}$  and  $^{31}\text{P}$  spectra at 15 °C, indicating a major enhancement in lipid disorder or rapidly diffusing lipid or tumbling structures. Caerin 1.1 (Fig. 3), however, did not promote an enhanced interaction with the lipid acyl chains, which were characteristic of a gel phase. The lipid headgroup region experienced reduced motions with the formation of an additional broad  $^{31}\text{P}$  CSA (Fig. 5c) similar to the ordered/immobilised phase observed with the pure lipid and a slight increase in the ~41 ppm CSA observed at the preceding temperature.

For the mixed lipid system with aurein 1.2, the  $^2\text{H}$  spectrum (Fig. 3) consisted of a mixture of a narrow isotropic signal, indicating widespread bilayer disruption, and a minor residual gel phase component. A bilayer phase was retained as well as considerably more disordered lipid relative to the control. A large  $^{31}\text{P}$  isotropic phase indicated aurein 1.2 caused a significant increase in disordered lipid or formation of small rapidly tumbling aggregates. With caerin 1.1, a gel phase  $^2\text{H}$  spectrum,

with a minor isotropic signal, and no major changes in the linewidth of the  $^{31}\text{P}$  CSA indicated that the majority of the lipid was relatively immobile and in a gel phase together with a small more disordered population.

To investigate whether the changes in lipid bilayer structure that occurred due to the reduction in temperature were reversible, the samples were reheated to their original temperature. In contrast to the freeze-thaw process during sample preparation, which takes place quickly, this process is slower and the NMR samples were kept for several hours at each temperature. Cycling back through the gel-fluid transition temperature to 30 °C allowed lamellar bilayer systems to be restored, although with aurein 1.2 these were in a more disordered state than initially observed. With aurein 1.2 in DMPC, the order parameters of the upper acyl chain increased slightly, while the lower acyl chain region was more perturbed (Fig. S1). A reduction in resolution prevented the individual deuterated methylene peaks from being resolved, which suggests an enhanced interaction (leading to reduction in  $T_2$  relaxation times) within the bilayer interior. The greatly perturbed isotropic  $^{31}\text{P}$  spectrum observed at 15 °C partially reformed into a considerably disordered bilayer phase (Fig. 4d). The original 37 ppm CSA (Table 2) was partially restored (20% of original signal) and a smaller, more disordered bilayer phase also formed, representing

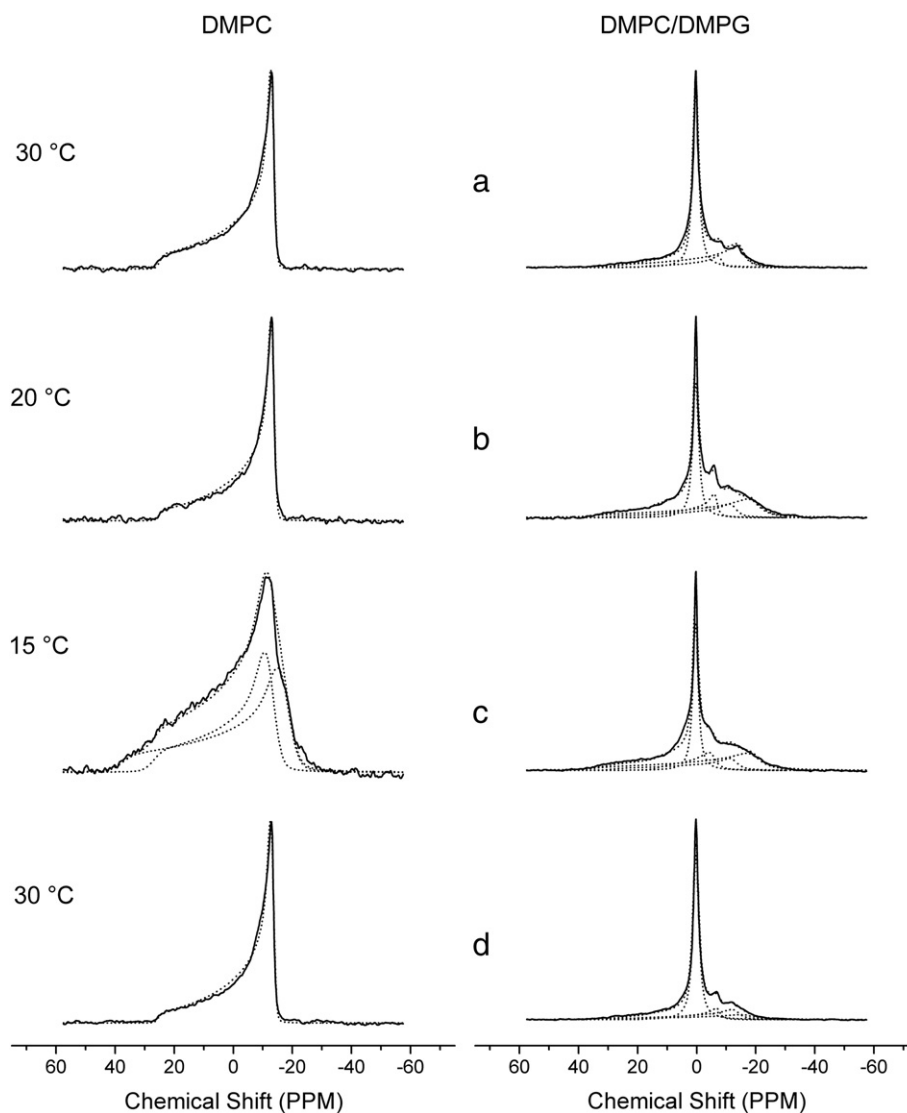


**Fig. 5.**  $^{31}\text{P}$  NMR spectra of DMPC (left) and DMPC/DMPG (2:1) (right) with caerin 1.1 at a 10:1 L/P ratio. Spectra were recorded (a) at 30 °C, (b) cooled to 20 °C, (c) further cooled to 15 °C, and (d) after reheated back to 30 °C. Unbroken lines represent the experimental spectra; dotted lines represent the deconvoluted components.

a greater level of disruption relative to the initial system. The large isotropic peak comprising 55% of the signal indicates that the temperature-induced disruptions to bilayer integrity are only partially reversible and that the temperature cycling assists peptide insertion into the bilayer. With caerin 1.1 in DMPC there was no significant change in the order parameter profile (Fig. S1) and the original  $^{31}\text{P}$  CSA was completely restored (Fig. 5d, Table 2), indicating that cycling through the phase transition did not cause any substantial effect on the interaction of the longer peptide.

For the mixed lipid system with aurein 1.2, reheating to 30 °C resulted in partial reformation of a more disordered mixed gel and fluid bilayer phase with considerable perturbation of the upper acyl chain segment (Table 2); which supports an enhanced surface interaction presumably driven by electrostatic attraction to the anionic lipid [55]. The  $^{31}\text{P}$  spectrum was largely restored although the individual CSAs were slightly broadened, indicating an increase in bilayer order, but an additional isotropic, more disordered, component (15%) was apparent (Table 2).

With caerin 1.1, the  $^2\text{H}$  spectrum returned to a complex mixture of gel, isotropic and disordered lamellar bilayer (Table 2). A broad ~55 ppm ordered/immobilised lipid phase together with two narrower, 37 and 25 ppm  $^{31}\text{P}$  CSAs, was present and the proportion of signal at the

isotropic chemical shift returned close to that observed initially, as the increase in temperature liberated some immobilised lipid.

#### 4. Discussion

In this study, solid-state NMR and CD spectroscopy were used to examine aurein 1.2 and caerin 1.1 in PC and PC/PG membrane systems to refine our understanding of their mode of action and lead to more effective AMP. The secondary structure adopted by aurein 1.2 and caerin 1.1 in neutral and anionic phospholipid membranes as well as the interaction with fluid and gel phase lipid bilayers are discussed.

##### 4.1. Mode of antimicrobial peptide interaction

The moderate decrease in the  $^{31}\text{P}$  CSA of DMPC at 30 °C (Table 2) observed with both peptides together with the observed changes in the  $^2\text{H}$  order parameter profiles and secondary structure (Table 1) suggests a different mode of action for each peptide. Together, the CD spectroscopy,  $^{31}\text{P}$  and  $^2\text{H}$  NMR data indicate that aurein 1.2 has a high propensity to form an  $\alpha$ -helix and interacts primarily with the neutral bilayer surface, consistent with previous studies [7,12,13], while the cryo-TEM and AFM images (Figs. S3 & S4b) show a breakdown of DMPC lipid

vesicles into smaller structures. Caerin 1.1 was more unstructured in the neutral lipid, increased disorder about the phospholipid headgroup and lower acyl chain region, while promoting a slight ordering effect in the upper acyl chain, consistent with a previous study [7]. No specific changes to the DMPC vesicles were observed by AFM (Fig. S4c) suggesting no overall changes to bilayer integrity. In contrast to the shorter peptide, these results are suggestive of peptide interaction throughout the entire bilayer due to peptide penetration.

Consistent with previous studies that emphasise the importance of membrane charge in modulating cationic AMP–membrane interactions [6,14,15,22,28,38,43,53], significant effects were observed on anionic phospholipid bilayers with both peptides. Aurein 1.2 had a similar propensity to form an  $\alpha$ -helix and perturbed the entire length of the acyl chain region with a significant narrowing of the DMPG CSA component. The effect is consistent with a primarily surface interaction and intercalation among the headgroup region, which would allow greater motional flexibility within the acyl chain region. While the mode of action of aurein 1.2 broadly reflected that seen with DMPC, caerin 1.1 had a more complex mode of interaction that led to the formation of a mixture of multiple lipid phases or domains in the anionic bilayer. Both CD and NMR showed that the peptide was more  $\alpha$ -helical in the presence of the anionic lipid and caused significant disruption of the lipid headgroup region and acyl chain interior, leading to the co-existence of gel, fluid and isotropic bilayer phases. Caerin 1.1 likely inserted into the bilayer, creating lipid domains of different acyl chain orders and inducing the formation of highly curved regions such as those in a toroidal pore model [17,19] (or highly curved structures as seen by AFM of vesicles on a solid surface, Fig. S4f). For both peptides, the significant interaction and formation of different lipid domains imply a preferential interaction for the anionic DMPG component.

#### 4.2. Influence of phospholipid phase on antimicrobial peptide activity

While the mode of action of each peptide has been observed in fluid phase membranes, the interaction was shown significantly to differ below the phase transition temperature of the pure lipids ( $\sim 23^\circ\text{C}$ ). The effect of the gel–fluid phase transition was investigated by performing the NMR measurements at 30, 20, and  $15^\circ\text{C}$  and then reheating to  $30^\circ\text{C}$ .

Reducing the temperature produced a ripple phase [34] in the DMPC bilayer, with interspersed areas of ordered and disordered phospholipid headgroups observed by  $^{31}\text{P}$  NMR, while the  $^2\text{H}$  NMR spectra were dominated by acyl chains in an ordered phase [56,57]. In the mixed lipid bilayers, however, the presence of the DMPG permitted a greater freedom of motion in the headgroup region such that the  $^{31}\text{P}$  spectrum changed little with the drop in temperature, likely due to an alteration in the electric charge allowing greater mobility and altering the orientation of the lipid headgroups [58]. While the headgroup region was more perturbed than for pure DMPC, the  $^2\text{H}$  spectra were consistent with gel phase lipid acyl chains suggesting that the disorder does not continue into the bilayer interior.

Lowering the temperature promoted a significant enhancement of the effect of aurein 1.2 on the neutral DMPC bilayer, while minimal additional effect was seen with the larger caerin 1.1 (Figs. 4b & 5b). The surface interaction of aurein 1.2 was enhanced at  $20^\circ\text{C}$ , just below the gel–fluid transition of the pure lipid, and the acyl chain interior continued to display characteristics of a fluid phase, consistent with AMP shifting the phase transition temperature [15]. The decrease in temperature may have enhanced peptide interaction due to the formation of defects in the mixed ordered/disordered ripple phase [29,34,35] or the more ordered acyl chains may facilitate the interaction [59]. These results are consistent with an enhanced lytic effect of aurein 1.2 and a related peptide, maculatin 1.1, observed below the lipid phase transition in QCM-D and DPI studies [36,37].

Whereas only aurein 1.2 showed enhanced interaction with the neutral DMPC at  $20^\circ\text{C}$ , in the mixed DMPC/DMPG bilayer both peptides did. For aurein 1.2, the lipid components became more intimately mixed as the  $^{31}\text{P}$  CSA components became more equal, while broadening of the linewidth reflected slower lipid motions. The large isotropic peak observed with caerin 1.1 reduced in intensity and an additional broad CSA formed, due to slower motions at the lower temperature. The transformation of the  $^2\text{H}$  spectrum into a mixed gel and isotropic phase was consistent with reduced lipid dynamics.

Further reduction in temperature to  $15^\circ\text{C}$  resulted in a complete disruption of the DMPC bilayer by aurein 1.2 into small, rapidly tumbling or diffusing aggregates. A similar effect was evident with the mixed lipid bilayer in which an enhanced interaction also led to formation of small rapidly tumbling or diffusing lipid aggregates, although a small amount of residual lamellar bilayer remained. In both cases the manner in which the lipid bilayers were disrupted was consistent with the carpet mechanism, with peptide interaction enhanced at the lower temperature. In contrast, at  $15^\circ\text{C}$  the larger caerin 1.1 did not display any enhanced interaction with DMPC relative to at  $20^\circ\text{C}$ , with only a general reduction of lipid motion observed. This was similar to the mixed lipid system in which no further changes were seen suggesting that the change in temperature and phase had little effect on the activity of the larger peptide. The enhanced effects of the smaller peptide are similar to those seen with other membrane lytic peptides such as melittin which induces formation of small 20–40 nm lipid discs in phospholipid bilayers after passing through the gel–fluid phase transition into the ripple and gel phase [29,33]. A reversible transition between disc-like micelles and extended bilayers occurs with temperature through the DMPC phase transition [31] and is driven by peptide interaction with defects formed in the gel and intermediate ripple phases. Cryo-TEM studies conducted with the diluted NMR samples revealed small lipid structures (Fig. S3), while AFM measurements (Fig. S4) also showed a disruption of the membrane consistent with aurein 1.2 adopting a similar mode of action. In a similar manner the AMP, magainin 2 [27] and maculatin 1.1 [26] also induce formation of isotropic  $^{31}\text{P}$  NMR signals in DMPC bilayers below the phase transition.

Apart from caerin 1.1 in DMPC, which had a minimal interaction that did not change with temperature cycling, each bilayer system was considerably more perturbed when returned back to the fluid phase at  $30^\circ\text{C}$ . For aurein 1.2 with DMPC and both peptides in the mixed lipid bilayers, additional disorder was present relative to the starting condition. However, for the bilayer with aurein 1.2 a large isotropic component was retained, suggesting that cycling through the phase transition enhanced the membrane disruption by the peptide. The acyl chain interior was more perturbed, which may have been due to peptide intercalating among the interfacial/upper acyl chain region and increasing the order parameters while allowing more freedom of motion and reduced order deeper in the bilayer. The mixed lipid bilayer continued to exhibit an isotropic phase with aurein 1.2 and the lipids present were more intimately mixed than before passing through the gel–liquid transition temperature. Caerin 1.1 with the mixed bilayer continued to exhibit characteristics of mixed gel, fluid and isotropic phases when returned to  $30^\circ\text{C}$ , suggesting that the peptide promoted domain formation. With the exception of DMPC with caerin 1.1, the slow passage through the phase transition enhanced the peptide interaction with the membrane.

In summary, both peptides gained significant  $\alpha$ -helical secondary structure in the presence of the DMPC membrane. In the fluid phase, aurein 1.2 displayed a primary surface interaction with eukaryotic-like bilayers, while the larger caerin 1.1 penetrated into and affected the full length of the bilayer. Both peptides interacted in a manner which significantly perturbed bilayer order, but retained overall bilayer integrity.

In the model prokaryotic-like bilayers, both peptides displayed a preferential interaction with the anionic DMPG component. Aurein



1.2 interacted with the interfacial region between the headgroup and acyl chain interior in a manner which enhanced disorder or motional flexibility within the bilayer core. Caerin 1.1 was able to penetrate into the bilayer interior and promoted the formation and stabilisation of a mixture of isotropic, gel and fluid phase lipid domains in a manner suggestive of toroidal pore formation.

Below the phase transition of eukaryotic-like bilayers, aurein 1.2 induced a complete bilayer disruption into small, rapidly tumbling lipid aggregates, similar to the effects of melittin [29,31–33] and maculatin 1.1 [26]. Caerin 1.1, however, did not display any enhanced interaction with the eukaryotic-like bilayer. Although a lamellar bilayer phase was largely retained for the prokaryotic-like bilayers, together with a significant isotropic phase for caerin 1.1, a partial disruption via the carpet mechanism was observed with aurein 1.2. The mode of action of aurein 1.2 was enhanced relative to the fluid phase and was likely driven by the co-existence of membrane defects. Caerin 1.1 did not display any significantly enhanced interaction at lower temperatures. The enhanced effects of aurein 1.2 in the gel phase show that the role of lipid phase and order needs to be considered when studying membrane interactions of AMPs and suggest that the lipid chains may also play a significant role in the selectivity of antimicrobial peptides.

## 5. Conclusions

The solid-state NMR data of aurein 1.2 and caerin 1.1 with model membranes above and below the gel–fluid transition temperature indicate that peptide activity and insertion is influenced by the phase/order of the membrane. The lipid compositions of bacterial membranes evolve during the growth cycle, substituting unsaturated and saturated species and, therefore, modulating fluid and gel phase properties. Hence, understanding the peptide activity in both phases is critical in their development as potent antibiotics in order to design AMP with high affinity and activity.

## Acknowledgements

DIF acknowledges the Australian government for receipt of an Australian Postgraduate Award (APA) and The University of Melbourne for receipt of an Albert Shimmins Postgraduate Writing-Up Award. FS thanks the Australian Research Council for financial support. MS was supported by a Royal Society travel grant (to BAW). The work at Birkbeck College was supported by a project grant from the UK Biotechnology & Biological Sciences Research Council (to BAW). The authors thank Dr Lynne Waddington (CSIRO, Australia) for her assistance with electron microscopy and Prof. Ka Yee Lee and Mr Michael Henderson (University of Chicago) for help with AFM measurements.

## Appendix A. Supplementary data

Supplementary data to this article can be found online at <http://dx.doi.org/10.1016/j.bbmem.2013.03.010>.

## References

- [1] M.A. Apponyi, T.L. Pukala, C.S. Brinkworth, V.M. Meselli, J.H. Bowie, M.J. Tyler, G.W. Booker, J. Wallace, J.A. Carver, F. Separovic, J. Doyle, L.E. Llewellyn, Host defence peptides of Australian anurans: structure, mechanism of action and evolutionary significance, *Peptides* 25 (2004) 1035.
- [2] T. Rozek, R.J. Waugh, S.T. Steinborner, J.H. Bowie, M.J. Tyler, J.C. Wallace, The maculatin peptides from the skin glands of the tree frog *Litoria genimaculata*: a comparison of the structures and antibacterial activities of maculatin 1.1 and caerin 1.1, *J. Pept. Sci.* 4 (1998) 111–115.
- [3] T.K. Rozek, L. Wegener, J.H. Bowie, I.N. Olver, J.A. Carver, J.C. Wallace, M.J. Tyler, The antibiotic and anticancer active aurein peptides from the Australian Bell Frogs *Litoria aurea* and *Litoria raniformis*. The solution structure of aurein 1.2, *Eur. J. Biochem.* 267 (2000) 5330–5341.
- [4] D.J.M. Stone, J.H. Bowie, M.J. Tyler, J.C. Wallace, The structure of caerin 1.1, a novel antibiotic peptide from Australian tree frogs, *J. Chem. Soc. Chem. Commun.* (1992) 1224–1225.
- [5] H. Wong, J.H. Bowie, J.A. Carver, The solution structure and activity of caerin 1.1, an antimicrobial peptide from the Australian green tree frog, *Litoria splendida*, *Eur. J. Biochem.* 247 (1997) 545–557.
- [6] D.I. Fernandez, J.D. Gehman, F. Separovic, Membrane interactions of antimicrobial peptides from Australian frogs, *Biochim. Biophys. Acta* 1788 (2009) 1630–1638.
- [7] I. Marcotte, K.L. Wegener, Y.-H. Lam, B.C.S. Chia, M.R.R.d. Planque, J.H. Bowie, M. Auger, F. Separovic, Interaction of antimicrobial peptides from Australian amphibians with lipid membranes, *Chem. Phys. Lipids* 122 (2003) 107–120.
- [8] K.L. Wegener, J.A. Carver, J.H. Bowie, The solution structures and activity of caerin 1.1 and caerin 1.4 in aqueous trifluoroethanol and dodecylphosphocholine micelles, *Biopolymers* 69 (2003) 42–59.
- [9] S.R. Dennison, F. Harris, D.A. Phoenix, The interactions of aurein 1.2 with cancer cell membranes, *Biophys. Chem.* 127 (2007) 78–83.
- [10] S.E. VanCompernelle, R.J. Taylor, K.O. Richter, J. Jiang, B.E. Youree, J.H. Bowie, M.J. Tyler, J.M. Conlon, D. Wade, C. Aiken, T.S. Dermody, V.N. KewelRamani, L.A. Rollins-Smith, D. Unutmaz, Antimicrobial peptides from amphibian skin potently inhibit human immunodeficiency virus infection and transfer of virus from dendritic cells to T cells, *J. Virol.* 79 (2005) 11598–11606.
- [11] G. Wang, K.M. Watson, A. Peterkofsky, R.W. Buckheit Jr., Identification of novel human immunodeficiency virus type 1-inhibitory peptides based on the antimicrobial peptide database, *Antimicrob. Agents Chemother.* 54 (2010) 1343–1346.
- [12] E.E. Ambroggio, F. Separovic, J.H. Bowie, G.D. Fidelio, L.A. Bagatolli, Direct visualisation of membrane leakage induced by the antibiotic peptides: maculatin, citropin, and aurein, *Biophys. J.* 89 (2005) 1874–1881.
- [13] M.S. Balla, J.H. Bowie, F. Separovic, Solid-state NMR study of antimicrobial peptides from Australian frogs in phospholipid membranes, *Eur. Biophys. J. Biophys. Lett.* 33 (2004) 109–116.
- [14] M. Boland, F. Separovic, Membrane interactions of antimicrobial peptides from Australian tree frogs, *Biochim. Biophys. Acta* 1758 (2006) 1178–1183.
- [15] G.W.J. Seto, S. Marwaha, D.M. Kobewka, R.N.A.H. Lewis, F. Separovic, R.N. McElhaney, Interactions of the Australian tree frog antimicrobial peptides aurein 1.2, citropin 1.1 and maculatin 1.1 with lipid model membranes: differential scanning calorimetric and Fourier transform infrared spectroscopic studies, *Biochim. Biophys. Acta* 1768 (2007) 2787–2800.
- [16] Z. Oren, Y. Shai, Mode of action of linear amphipathic  $\alpha$ -helical antimicrobial peptides, *Biopolymers (Pept. Sci.)* 47 (1999) 451–463.
- [17] Y. Shai, Mechanism of the binding, insertion and destabilisation of phospholipid bilayer membranes by  $\alpha$ -helical antimicrobial and cell non-selective membrane lytic peptides, *Biochim. Biophys. Acta* 1462 (1999) 55–70.
- [18] Y. Shai, Z. Oren, From “carpet” mechanism to de-novo designed diastereomeric cell-selective antimicrobial peptides, *Peptides* 22 (2001) 1629–1641.
- [19] L. Yang, T.A. Harroun, T.M. Weiss, L. Ding, H.W. Huang, Barrel-stave model or toroidal model? A case study on melittin pores, *Biophys. J.* 81 (2001) 1475–1485.
- [20] Y. Shai, Mode of action of membrane active antimicrobial peptides, *Biopolymers* 66 (2002) 236–248.
- [21] D.I. Fernandez, A.P.L. Brun, T.C. Whitwell, M.-A. Sani, M. James, F. Separovic, The antimicrobial peptide aurein 1.2 disrupts model membranes via the carpet mechanism, *Phys. Chem. Chem. Phys.* 14 (2012) 15739–15751.
- [22] K.N. Hall, H. Mozsolits, M.-I. Aguilar, Surface plasmon resonance analysis of antimicrobial peptide–membrane interactions: affinity & mechanism of action, *Lett. Pept. Sci.* 10 (2003) 475–485.
- [23] A.I.P.M. de Kroot, Metabolism of phosphatidylcholine and its implications for lipid acyl chain composition in *Saccharomyces cerevisiae*, *Biochim. Biophys. Acta Mol. Cell Biol. Lipids* 1771 (2007) 343–352.
- [24] F.D. Gunstone, J.L. Harwood, Occurrence and characterisation of oils and fats, in: F.D. Gunstone, J.L. Harwood, A.J. Dijkstra (Eds.), *The Lipids Handbook*, CRC Press, Taylor and Francis Group, 2007, pp. 37–141.
- [25] D.E. Warschawski, A.A. Arnold, M. Beauprand, A. Gravel, É. Chartrand, I. Marcotte, Choosing membrane mimetics for NMR structural studies of transmembrane proteins, *Biochim. Biophys. Acta* 1808 (2011) 1957–1974.
- [26] D.I. Fernandez, T.-H. Lee, M.-A. Sani, M.-I. Aguilar, F. Separovic, Proline facilitates the membrane insertion of the antimicrobial peptide maculatin 1.1 via surface indentation and subsequent lipid disordering, *Biophys. J.* (2013), <http://dx.doi.org/10.1016/j.bpj.2013.01.059> (in press).
- [27] B. Bechinger, Detergent-like properties of magainin antibiotic peptides: a  $^{31}\text{P}$  solid-state NMR spectroscopy study, *Biochim. Biophys. Acta* 1712 (2005) 101–108.
- [28] B. Bechinger, K. Lohner, Detergent-like actions of linear amphipathic cationic antimicrobial peptides, *Biochim. Biophys. Acta* 1758 (2006) 1529–1539.
- [29] T. Pott, J. Dufourcq, E.J. Dufourcq, Fluid or gel phase lipid bilayers to study peptide–membrane interactions? *Eur. Biophys. J.* 25 (1996) 55–59.
- [30] F. Dupuy, R. Morero, Microcin J25 membrane interaction: selectivity towards gel phase, *Biochim. Biophys. Acta* 1808 (2011) 1764–1771.
- [31] C.E. Dempsey, B. Sternberg, Reversible disc-micellization of dimyristoylphosphatidylcholine bilayers induced by melittin and [Ala-14] melittin, *Biochim. Biophys. Acta* 1061 (1991) 175–184.
- [32] E.J. Dufourcq, I.C.P. Smith, J. Dufourcq, Molecular details of melittin-induced lysis of phospholipid membranes as revealed by deuterium and phosphorus NMR, *Biochemistry* 25 (1986) 6448–6455.
- [33] T. Pott, E.J. Dufourcq, Action of melittin on the DPPC-cholesterol liquid-ordered phase: a solid state  $^2\text{H}$ - and  $^{31}\text{P}$ -NMR study, *Biophys. J.* 68 (1995) 965–977.
- [34] M. Kranenburg, B. Smit, Phase behavior of model lipid bilayers, *J. Phys. Chem. B* 109 (2005) 6553–6563.
- [35] D. Ruppel, H.-G. Kapitza, H.J. Galla, F. Sixl, E. Sackmann, On the microstructure and phase diagram of dimyristoylphosphatidylcholine-glycophorin bilayers, *Biochim. Biophys. Acta* 692 (1982) 1–17.

- [36] A. Mechler, S. Praporski, K. Atmuri, M. Boland, F. Separovic, L.L. Martin, Specific and selective peptide-membrane interactions revealed using quartz crystal microbalance, *Biophys. J.* 93 (2007) 3907–3916.
- [37] T.-H. Lee, C. Heng, M.J. Swann, J.D. Gehman, F. Separovic, M.-I. Aguilar, Real-time quantitative analysis of lipid disordering by aurein 1.2 during membrane adsorption, destabilisation and lysis, *Biochim. Biophys. Acta* 1798 (2010) 1977–1986.
- [38] J.D. Gehman, F. Luc, K. Hall, T.-H. Lee, M.P. Boland, T.L. Pukala, J.H. Bowie, M.I. Aguilar, F. Separovic, Effect of antimicrobial peptides from Australian tree frogs on anionic phospholipid membranes, *Biochemistry* 47 (2008) 8557–8565.
- [39] M.-A. Sani, C. Loudet, G. Grobner, E.J. Dufourc, Pro-apoptotic Bax- $\alpha$  1 synthesis and evidence for  $\beta$ -sheet to  $\alpha$ -helix conformational change as triggered by negatively charged lipid membranes, *J. Pept. Sci.* 13 (2007) 100–106.
- [40] M.H. Levitt, Composite pulses, *Prog. Nucl. Magn. Reson. Spectrosc.* 18 (1986) 61–122.
- [41] J.H. Davis, M. Bloom, K.W. Butler, I.C. Smith, The temperature dependence of molecular order and the influence of cholesterol in *Acholeplasma laidlawii* membranes, *Biochim. Biophys. Acta* 597 (1980) 477–491.
- [42] M. Rance, R.A. Byrd, Obtaining high-fidelity spin 1/2 powder spectra in anisotropic media: phase-cycled Hahn echo spectroscopy, *J. Magn. Reson.* 52 (1983) 221–240.
- [43] D.I. Fernandez, M.-A. Sani, F. Separovic, Interactions of the antimicrobial peptide maculatin 1.1 and analogues with phospholipid bilayers, *Aust. J. Chem.* 64 (2011) 798–805.
- [44] L. Whitmore, B.A. Wallace, Protein secondary structure analyses from circular dichroism spectroscopy: methods and reference databases, *Biopolymers* 89 (2008) 392–400.
- [45] A. Abdul-Gader, A.J. Miles, B.A. Wallace, A reference dataset for the analyses of membrane protein secondary structures and transmembrane residues using circular dichroism spectroscopy, *Bioinformatics* 27 (2011) 1630–1636.
- [46] N. Sreerama, R.W. Woody, Estimation of protein secondary structure from circular dichroism spectra: comparison of CONTIN, SELCON, and CDSSTR methods with an expanded reference set, *Anal. Biochem.* 287 (2000) 252–260.
- [47] A.J. Miles, L. Whitmore, B.A. Wallace, Spectral magnitude effects on the analyses of secondary structure from circular dichroism spectroscopic data, *Protein Sci.* 14 (2005) 368–374.
- [48] J.R. Silvius, Thermotropic phase transitions of pure lipids in model membranes and their modifications by membrane proteins, *Lipid-Protein Interactions*, John Wiley & Sons, New York, 1982.
- [49] J. Seelig, W. Niederberger, Deuterium-labelled lipids as structural probes in liquid crystalline bilayers. A deuterium magnetic resonance study, *J. Am. Chem. Soc.* 96 (1974) 2069–2072.
- [50] P.R. Cullis, B.d. Kruijff, Lipid polymorphism and the functional roles of lipids in biological membranes, *Biochim. Biophys. Acta* 559 (1979) 399–420.
- [51] J. Seelig,  $^{31}\text{P}$  nuclear magnetic resonance and the head group structure of phospholipids in membranes, *Biochim. Biophys. Acta* 515 (1978) 105–140.
- [52] P.J. Sherman, R.J. Jackway, J.D. Gehman, S. Praporski, G.A. McCubbin, A. Mechler, L.L. Martin, F. Separovic, J.H. Bowie, The solution structure and membrane interactions of the antimicrobial peptide fallaxidin 4.2: an NMR and QCM study, *Biochemistry* 48 (2009) 11892–11901.
- [53] D.I. Fernandez, M.-A. Sani, J.D. Gehman, K.-S. Hahn, F. Separovic, Interactions of a synthetic Leu-Lys-rich antimicrobial peptide with phospholipid bilayers, *Eur. Biophys. J. Biophys. Lett.* 40 (2011) 471–480.
- [54] J.F. Nagle, S. Tristram-Nagle, Structure of lipid bilayers, *Biochim. Biophys. Acta Rev. Biomembr.* 1469 (2000) 159–195.
- [55] M.-A. Sani, T.C. Whitwell, F. Separovic, Lipid composition regulates the conformation and insertion of the antimicrobial peptide maculatin 1.1, *Biochim. Biophys. Acta Biomembr.* 1818 (2012) 205–211.
- [56] K. Schorn, D. Marsh, Dynamic chain conformations in dimyristoyl glyceroldimyristoylphosphatidylcholine mixtures.  $^2\text{H}$ -NMR studies, *Biophys. J.* 71 (1996) 3320–3329.
- [57] M.R. Vist, J.H. Davis, Phase equilibria of cholesterol/dipalmitoylphosphatidylcholine mixtures:  $^2\text{H}$  nuclear magnetic resonance and differential scanning calorimetry, *Biochemistry* 29 (1990) 451–464.
- [58] P.G. Scherer, J. Seelig, Electric charge effects on phospholipid headgroups. Phosphatidylcholine in mixtures with cationic and anionic amphiphiles, *Biochemistry* 28 (1989) 7720–7728.
- [59] K.A. Henzler-Wildman, G.V. Martinez, M.F. Brown, A. Ramamoorthy, Perturbation of the hydrophobic core of lipid bilayers by the human antimicrobial peptide LL-37, *Biochemistry* 43 (2004) 8459–8469.